

Numerical Studies of Laminar Flame Propagation in Spherical Bombs

J. I. Ramos*

Carnegie-Mellon University, Pittsburgh, Pennsylvania

A reaction-diffusion equation which has an exact traveling wave solution is used to characterize the accuracy of nine finite difference schemes. These schemes are then applied to study the propagation of a laminar flame in a spherical bomb where chemistry is modeled by a one-step Arrhenius-type reaction. The numerical schemes evaluated include an implicit predictor-corrector method, a quasilinear algorithm, a majorant operator splitting technique, two methods of lines, a linear block tridiagonal procedure, and the standard explicit, implicit, and Crank-Nicolson methods. The numerical results indicate that the most accurate scheme is the fourth-order method of lines whose efficiency is comparable to that of the most efficient explicit algorithm.

Nomenclature

A	= vector defined by Eq. (25) or scalar defined by Eq. (49)
C_p	= specific heat at constant pressure, $C_p = 7$ cal/mole/K
C_v	= specific heat at constant volume
E	= activation energy, = 30,000 cal/mole
H^0	= enthalpy of formation
h	= space step, = $\xi_{i+1} - \xi_i$
I	= unit matrix
K	= pre-exponential factor, = 3.12×10^{11} cm ³ /g/s
L	= diffusion operator defined by Eq. (32)
m, n	= exponents defined in Eq. (48)
\dot{m}	= reaction rate
M	= mass contained in the spherical bomb
N	= number of species, = 4
p	= pressure
Q	= heat of reaction, = 11,070 cal/g
r	= radial location
\bar{R}	= universal gas constant
R	= spherical bomb radius, = 10 cm
s	= stoichiometric coefficient, = 3.63
S	= reaction terms defined by Eq. (27)
t	= time
u	= radial velocity
V	= wave speed
W	= molecular weight, = 28.91 g/mole
Y	= species mass fractions
α	= $\rho\mu/M^2$
β, δ	= coefficients in Eq. (48)
γ	= ratio of specific heats, = 1.4
Δt	= time step
μ	= dynamic viscosity
ξ	= Lagrangian coordinate defined by Eqs. (10) and (11)
ρ	= density, $\rho\mu = 2.1718 \times 10^{-7}$ g ² /cm ⁴ /s
ϕ	= variable defined by Eq. (7)
Superscripts	
k	= iteration within the time step
$n, n+1$	= previous and actual times
$(-)$	= predicted quantities

Subscripts

c	= computed
d	= diffusion
i	= grid point
j	= species
R	= reaction

Introduction

THE purpose of this paper is to assess the relative efficiency and accuracy of nine finite difference schemes in the numerical solution of laminar flame propagation problems in a spherical bomb. The efficiency is evaluated in terms of the computational time required to achieve a certain accuracy and is assessed for only one set of chemical reaction data and one geometrical configuration. The accuracy of the numerical methods is evaluated in terms of the pressure values at several times, when the same time step is used in all the numerical schemes. The numerical methods also are compared in terms of truncation errors for a simple nonlinear reaction-diffusion equation which has an exact traveling wave solution. The accuracy of the calculations is assessed here by comparing the computed and exact steady-state wave speeds.

A similar assessment of numerical efficiency and accuracy has also been conducted by Reitz,¹ who studied one-dimensional unsteady reaction-diffusion equations. Otey and Dwyer² assessed the accuracy of an operator splitting algorithm, two method of lines techniques, a linear block scheme, and a method of lines in the numerical calculation of the steady-state wave speed of a reaction-diffusion equation. Their results show that the linear block method with fourth-order spatial differences is the most efficient one over a wide range of reaction rates. For confined laminar flames, Ramos³ has shown that the explicit method is more efficient than other methods such as implicit schemes, method of lines, operator splitting, and linear block algorithms. These studies indicate that efficiency and accuracy are sensitive to the geometrical arrangement, e.g., confinement or unconfinement. They are also sensitive to the problem dimensionality and nonlinearity.

In this paper the propagation of confined spherical flames is formulated in such a way that the momentum and overall mass conservation equations need not be considered. This and other simplifications reduce the governing equations to a system of nonlinear integrodifferential reaction-diffusion equations. Since the emphasis here is on evaluating the accuracy and efficiency of various numerical methods rather than on predicting hydrocarbon combustion or flame speeds, a simple one-step Arrhenius-type reaction has been used in the calculations.

Presented as Paper 82-0038 at the AIAA 20th Aerospace Sciences Meeting, Orlando, Fla., Jan. 11-14, 1982; submitted Jan. 20, 1982; revision received May 25, 1982. Copyright © American Institute of Aeronautics and Astronautics, Inc., 1982. All rights reserved.

*Assistant Professor, Department of Mechanical Engineering. Member AIAA.

Governing Equations

The conservation equations for multidimensional reacting ideal mixtures can be found in Williams.⁴ These equations can be simplified by assuming spherical symmetry and by neglecting the thermal diffusion of the species (i.e., the Soret and Dufour effects), the pressure gradient diffusion, the bulk viscosity, and radiation heat transfer. Furthermore, in enclosed deflagrations, the Mach number is small and the pressure is almost spatially uniform, i.e., $p = p(t)$. Under this assumption the momentum equation and the viscous dissipation terms can be disregarded. Assuming that the species diffuse according to Fick's law with equal mass diffusivities, the Prandtl, Lewis, and Schmidt numbers are each equal to one, and equal specific heats at constant pressure, the equations governing the propagation of laminar flames in a spherical bomb can be written as follows.

Continuity:

$$\frac{\partial \rho}{\partial t} + \frac{1}{r^2} \frac{\partial}{\partial r} [\rho r^2 u] = 0 \quad (1)$$

Momentum:

$$p = p(t) \quad (2)$$

Energy:

$$\rho C_p \left[\frac{\partial T}{\partial t} + u \frac{\partial T}{\partial r} \right] = \frac{dp}{dt} + \frac{1}{r^2} \frac{\partial}{\partial r} \left[r^2 \mu C_p \frac{\partial T}{\partial r} \right] - \sum_{j=1}^N H_j^0 \dot{m}_j \quad (3)$$

Species:

$$\rho \left[\frac{\partial Y_j}{\partial t} + u \frac{\partial Y_j}{\partial r} \right] = \dot{m}_j + \frac{1}{r^2} \frac{\partial}{\partial r} \left[\mu r^2 \frac{\partial Y_j}{\partial r} \right] \quad j=1, \dots, N-1 \quad (4)$$

$$Y_N = 1 - \sum_{j=1}^{N-1} Y_j \quad (5)$$

State:

$$p = \bar{R} T \sum_{j=1}^N \frac{Y_j}{W_j} \quad (6)$$

Equations (1-6) can be further simplified by assuming that the specific heats at constant pressure and at constant volume are constant. This means that the ratio of specific heats, $\gamma = C_p/C_v$, is also a constant. These assumptions allow us to introduce the following transformation:

$$\phi = T p^{(1-\gamma)/\gamma} \quad (7)$$

which when substituted into Eqs. (3) and (6) yields

$$\rho C_p p^{(\gamma-1)/\gamma} \left[\frac{\partial \phi}{\partial t} + u \frac{\partial \phi}{\partial r} \right] = C_p p^{(\gamma-1)/\gamma} \frac{1}{r^2} \frac{\partial}{\partial r} \left[\mu r^2 \frac{\partial \phi}{\partial r} \right] - \sum_{j=1}^N H_j^0 \dot{m}_j \quad (8)$$

and

$$p^{(1/\gamma)} = \rho \frac{\bar{R}}{W} \phi \quad (9)$$

Equations (1), (4), and (8) can be further simplified by introducing the following Lagrangian coordinates:

$$\rho r^2 = M \frac{\partial \xi}{\partial t} \quad (10)$$

and

$$\rho r^2 u = -M \frac{\partial \xi}{\partial t} \quad (11)$$

where

$$M = \int_0^R \rho r^2 dr \quad (12)$$

Equations (10) and (11) represent a mapping $(r, t) \rightarrow [\xi(r, t), t]$ where $0 \leq \xi \leq 1$, $t > 0$, and $0 \leq r \leq R$. Substituting Eqs. (10) and (11) into Eqs. (4) and (8) and assuming that $\alpha = \rho \mu / M^2$ is constant, i.e., $\rho \mu$ is constant, we derive the following equations.

$$\frac{\partial \phi}{\partial t} = \alpha \frac{\partial}{\partial \xi} \left[r^2 \frac{\partial \phi}{\partial \xi} \right] - \frac{\sum_{j=1}^N H_j^0 \dot{m}_j}{\rho C_p p^{(\gamma-1)/\gamma}} \quad (13)$$

$$\frac{\partial Y_j}{\partial t} = \alpha \frac{\partial}{\partial \xi} \left[r^2 \frac{\partial Y_j}{\partial \xi} \right] + \frac{\dot{m}_j}{\rho} \quad j=1, \dots, N-1 \quad (14)$$

$$Y_N = 1 - \sum_{j=1}^{N-1} Y_j \quad (15)$$

Equation (10) can be integrated with respect to r to yield

$$\frac{r^3}{3} = M \int_0^\xi \frac{d\xi}{\rho} = \frac{M \bar{R}}{W p^{(1/\gamma)}} \int_0^\xi \phi d\xi \quad (16)$$

which gives the value of r . The velocity u can be calculated from Eq. (1) as follows.

$$u = -\frac{1}{\rho r^2} \int_0^r r^2 \frac{\partial \rho}{\partial t} dr \quad (17)$$

This expression can be simplified using Eq. (10) to yield the following expression:

$$u = \frac{M}{r^2} \int_0^\xi \frac{\partial}{\partial t} \left(\frac{1}{\rho} \right) d\xi \quad (18)$$

The pressure can be calculated by integrating Eq. (9) across the combustor from $r=0$ to $r=R$ and using Eq. (10) to give

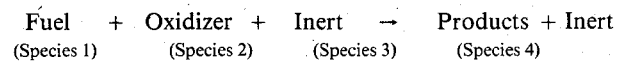
$$p^{(1/\gamma)} \frac{R^3}{3} = \frac{\bar{R}}{W} \int_0^R \rho \phi r^2 dr = \frac{M \bar{R}}{W} \int_0^1 \phi d\xi \quad (19)$$

The temperature and density are then calculated using Eqs. (7) and (9) respectively.

Equations (13) and (14) are reaction-diffusion equations with nonconstant, nonlinear diffusion coefficients. The nonlinearities arise due to dependence of r and p on ϕ through Eqs. (16) and (19).

Chemical Reaction

The chemical reaction terms appearing in Eqs. (13) and (14) have been modeled by a one-step Arrhenius-type reaction which can be written as



where the reaction rates are

$$\dot{m}_1 = K \exp \left(-\frac{E}{RT} \right) \rho^2 Y_1 Y_2 \quad (20)$$

$$\dot{m}_2 = -s K \exp \left(-\frac{E}{RT} \right) \rho^2 Y_1 Y_2 \quad (21)$$

$$\dot{m}_3 = 0 \quad (22)$$

$$\dot{m}_4 = -\dot{m}_1 - \dot{m}_2 \quad (23)$$

For an initially uniform distribution of the inert species, its mass fraction, Y_3 , remains constant in space and time, thus we have to solve only the equations governing the conservation of mass fractions of fuel and oxidizer since the mass fraction of products, Y_4 , is given by the conservation of mass fractions, Eq. (15). Furthermore, Eqs. (20) and (21) allow us to write the heat release term of Eq. (3) as follows:

$$\sum_{j=1}^N H_j^0 \dot{m}_j = Q \dot{m}_1 \quad (24)$$

where Q is the heat of reaction.

Substituting Eqs. (20), (21), and (24) into Eqs. (13) and (14), we can write the following vector equation:

$$\frac{\partial A}{\partial t} = \alpha \frac{\partial}{\partial \xi} \left[r^4 \frac{\partial A}{\partial \xi} \right] + S \quad (25)$$

where

$$A = (Y_1, Y_2, \phi)^T \quad (26)$$

and

$$S = \left(\frac{\dot{m}_1}{\rho}, \frac{\dot{m}_2}{\rho}, \frac{Q \dot{m}_1}{\rho C_p p^{(\gamma-1)/\gamma}} \right)^T \quad (27)$$

Equation (25) is to be solved subject to appropriate initial and boundary conditions.

In the present calculations, the spherical bomb was assumed to be adiabatic and the following boundary conditions applied.

$$\frac{\partial A}{\partial \xi} (0, t) = \frac{\partial A}{\partial \xi} (1, t) = 0 \quad (28)$$

Initially, the pressure was equal to 1 atm and the temperature and species mass fraction profiles were specified as follows.

$$Y_3(\xi, 0) = 0.69978 \quad 0 \leq \xi \leq 1 \quad (29)$$

$$T(\xi, 0) = 1500 \text{ K} \quad Y_1(\xi, 0) = 0.01 \quad Y_2(\xi, 0) = 0.03652 \quad 0 \leq \xi \leq 0.0438 \quad (30)$$

$$T(\xi, 0) = 300 \text{ K} \quad Y_1(\xi, 0) = 0.06472 \quad Y_2(\xi, 0) = 0.23550 \quad 0.0938 \leq \xi \leq 1 \quad (31)$$

Linear temperature and species mass fraction profiles were used for $0.0438 \leq \xi \leq 0.0938$.

It is worth noticing that Eq. (25) represents a system of integrodifferential reaction-diffusion equations.

Description of Numerical Methods

The choice of a numerical method for a system of coupled integrodifferential reaction-diffusion equations [Eq. (25)] is strongly influenced by the exponential nature of the nonlinear reaction terms [Eq. (20)], the nonlinear diffusion coefficient, r^4 , and the steep temperature and species mass fraction profiles which exist at the flame front. Thus, the formulation of a solution technique in which the reaction terms can be integrated point-by-point seems to offer a promising approach. This will be a basic ingredient in the method of lines, the explicit method of lines, and the majorant operator splitting techniques discussed subsequently. A point-by-point integration scheme of the highly nonlinear reaction terms is

also used in the implicit predictor-corrector method. Quasilinear and linear block tridiagonal algorithms are also used to study laminar flame propagation phenomena in a spherical bomb. These two methods are based on a linearization of the highly nonlinear reaction terms around the previous time. The other three methods studied here are the standard explicit, implicit, and Crank-Nicolson schemes.

The steepness of the temperature and species mass fraction profiles plays a critical role in the numerical solution of laminar flame propagation in spherical bombs. Therefore, spatial approximations and grid size are as important as the treatment of the temporal portion of the equations. In this paper, however, only second-order accurate spatial approximations are used. In these approximations a staggered grid has been employed and the diffusion terms have been discretized in an equally-spaced grid as follows:

$$L_d(A_i) = \alpha \frac{\partial}{\partial \xi} \left[r^4 \frac{\partial A}{\partial \xi} \right] \approx \frac{\alpha}{h} \left[\left(r^4 \frac{\partial A}{\partial \xi} \right)_{i+1/2} - \left(r^4 \frac{\partial A}{\partial \xi} \right)_{i-1/2} \right] \quad (32)$$

where

$$r_{i+1/2} = (r_i + r_{i+1})/2 \quad (33)$$

and

$$\left(\frac{\partial A}{\partial \xi} \right)_{i+1/2} = \frac{A_{i+1} - A_i}{h} \quad (34)$$

Method of Lines

The basic idea in the method of lines is to replace the spatial derivatives with an appropriate approximation which relates the dependent variables at neighboring grid points. This results in the following set of ordinary differential equations.

$$\frac{dA_i}{dt} = L_d(A_i) + S_i \quad (35)$$

These equations are written at each grid point. For a grid with M points, this procedure reduces the system of three partial differential equations [Eq. (25)] to a system of $3M$ coupled first-order ordinary differential equations which have been solved using a fourth-order accurate Runge-Kutta method. Unfortunately, Eq. (35) which gives the solution at grid point i , A_i , involves the unknown values of A at $i-1$ and $i+1$, through Eq. (32). This disadvantage is avoided in the explicit method of lines which is discussed next.

Explicit Method of Lines

The explicit method of lines is a simple technique based on the method of lines described above. This technique evaluates the diffusion terms, $L_d(A_i)$, explicitly at the previous time step as follows.

$$\frac{dA_i}{dt} = L_d(A_i^{(n)}) + S_i \quad (36)$$

Equation (36) yields the solution at $t^{(n+1)}$ and only involves the unknown values of the variables at the i th grid point. The resulting system of Eq. (36) was solved by a fourth-order accurate Runge-Kutta method. Although the explicit method of lines is a very simple technique, it suffers from two major disadvantages. First, because of the explicit evaluation of the diffusion terms, the integration of Eq. (36) has to be interrupted to re-evaluate the spatial derivatives frequently enough to satisfy the stability limitation imposed by the explicit evaluation of the diffusion terms. Second, both the method of lines and the explicit method of lines have the obvious disadvantage that they yield a large set of coupled

equations; however, they have the advantage of evaluating the reaction terms point by point.

Majorant Operator Splitting Method

This technique was originally proposed by Yannenkov⁵ and allows one term of Eq. (25) to be considered alone during each fractional step, while the remaining terms are ignored. In this study, a sequence of two fractional steps has been used.

1) Reaction step:

$$\frac{dA_i}{dt} = S_i \quad (37)$$

which has been solved using a fourth-order accurate Runge-Kutta method.

2) Diffusion step:

$$\frac{dA_i}{dt} = L_d(A_i) \quad (38)$$

The diffusion step was discretized using a second-order Crank-Nicolson scheme to yield

$$A_i^{(n+1)} - \bar{A}_i = \frac{\Delta t}{2} [L_d(\bar{A}_i) + L_d(A_i^{(n+1)})] \quad (39)$$

where the bar designates the values calculated in the reaction step. Equation (39) represents a tridiagonal matrix which was solved for the values of the dependent variables at $t^{(n+1)}$ by the well-known method of Thomas.⁶ It is to be noted that the computation has been carried out by first integrating Eq. (37) over a time interval $\Delta t = t^{(n+1)} - t^{(n)}$. During this process, the time step used in the integration of the reaction step was varied as necessary to maintain a specified accuracy and was generally smaller than Δt . The majorant operator splitting method retains the advantage of evaluating the reaction terms [Eq. (37)] point by point. Another advantage is that the diffusion operator has the stability characteristics normally associated with implicit methods. However, the accuracy of the operator splitting method depends very much on the time step and grid size. Obviously large time steps will uncouple the diffusion and reaction processes, producing significant errors and eventually instability.

Implicit Predictor-Corrector Method

This algorithm is similar to the explicit predictor-corrector methods. The difference arises from its implicit character. The basic idea of the method consists of predicting the value of the highly nonlinear terms S [Eq. (25)] implicitly and then use these values to evaluate the solution at the new time step. In this study the explicit method of lines was used in the predictor step as follows:

$$\frac{dA_i}{dt} = L_d(A_i^{(n)}) + S_i \quad (40)$$

while the corrector step used a kind of Crank-Nicolson scheme which can be written as

$$A_i^{(n+1)} - A_i^{(n)} = \frac{\Delta t}{2} [L_d(A_i^{(n)}) + L_d(A_i^{(n+1)})] + \frac{\Delta t}{2} [S_i^{(n)} + \bar{S}_i] \quad (41)$$

where \bar{S}_i stands for the value of the reaction terms evaluated with the solution obtained in the predictor step. The predictor step was evaluated using a fourth-order accurate Runge-Kutta method. The corrector step is almost a Crank-Nicolson scheme, except that the reaction terms $S_i^{(n+1)}$ have been replaced by the known reaction term \bar{S}_i .

Quasilinear Method

Equation (25) represents a system of coupled nonlinear partial differential equations which may be easy to solve if they are linearized in some way. In this section we will use the time quasilinearization technique first introduced by Bellman and Kalaba.⁷ This technique linearizes the reaction terms using a Taylor series expansion with respect to only that variable whose equation is being solved. The expansion of the variables is performed in time and around the previously known value. This time linearization is different from iteration quasilinearization, where the nonlinear terms are "quasilinearized" with respect to the values obtained in the previous iteration.⁷ In this study, a second-order accurate Crank-Nicolson scheme has been used to solve Eq. (25) as follows:

$$A_i^{(n+1)} - A_i^{(n)} = \frac{\Delta t}{2} [L_d(A_i^{(n)}) + L_d(A_i^{(n+1)})] + \frac{\Delta t}{2} [S_i^{(n)} + S_i^{(n+1)}] \quad (42)$$

where

$$S^{(n+1)} = S^{(n)} + \left(\frac{\partial S}{\partial A} \right)^{(n)} I (A^{(n+1)} - A^{(n)}) \quad (43)$$

and I is the unit matrix which when premultiplied by the Jacobian matrix $(\partial S / \partial A)^{(n)}$ yields a diagonal matrix. Mathematically, this means that $S^{(n+1)}$ is linearized with respect to only that variable whose equation is being solved. The advantage of the quasilinear method is to reduce the system of nonlinear coupled partial differential equations to a system of uncoupled linear partial differential equations. Unfortunately, in the present study this is not possible because p depends on a definite integral of ϕ through Eq. (19). The attractiveness of the quasilinear method is thus lost and iterations are required to account for the dependence of p and r on ϕ .

Linear Block Tridiagonal Algorithm

This algorithm has been used by Briley and McDonald⁸ and is based on the quasilinear method described earlier. The method uses the Crank-Nicolson form of Eq. (42); however Eq. (43) is now written in the following way.

$$S^{(n+1)} = S^{(n)} + \left(\frac{\partial S}{\partial A} \right)^{(n)} (A^{(n+1)} - A^{(n)}) \quad (44)$$

Thus, the nonlinear terms are linearized with respect to all the dependent variables. The resulting block tridiagonal matrix has been solved using lower-upper decomposition. The prime objective of the block method is to reduce the system of coupled nonlinear partial differential equations to a system of coupled linear equations, i.e., all the equations are coupled during the solution procedure. Unfortunately, as with the quasilinear method, the advantages of linearization are lost in the present study due to the fact that the pressure depends on ϕ [Eq. (19)]. As a result, the block method requires iterations. Both the quasilinear and block methods have the stability characteristics associated with implicit methods, however, their accuracy reduces as larger time steps are taken due to the linearization of the highly nonlinear reaction terms.

Explicit Method

The following first-order explicit method was used.

$$A_i^{(n+1)} - A_i^{(n)} = \Delta t L_d(A_i^{(n)}) + \Delta t S_i^{(n)} \quad (45)$$

Implicit Method

The following first-order implicit scheme was employed.

$$A_i^{(n+1)} - A_i^{(n)} = \Delta t L_d(A_i^{(n+1)}) + \Delta t S_i^{(n+1)} \quad (46)$$

Equation (46) was solved iteratively using the tridiagonal algorithm known as method of Thomas,⁶ without any relaxation or linearization.

Crank-Nicolson Scheme

The standard Crank-Nicolson finite difference equations

$$A_i^{(n+1)} - A_i^{(n)} = \frac{\Delta t}{2} [L_d(A_i^{(n)}) + L_d(A_i^{(n+1)})] + \frac{\Delta t}{2} [S_i^{(n)} + S_i^{(n+1)}] \quad (47)$$

were solved iteratively using the method of Thomas without any relaxation or linearization. It should be pointed out that the radial location and the pressure, Eqs. (16) and (19), were calculated using the trapezoidal rule in all the numerical methods investigated.

Presentation and Discussion of Results

The numerical methods discussed earlier have been applied first to compute the steady-state wave speed of a reaction-diffusion equation and then used to study the propagation of a laminar flame in a spherical bomb. These computations are discussed in the next two sections.

A Reaction-Diffusion Equation with an Exact Traveling Wave Solution

The propagation of a laminar flame in Cartesian coordinates was studied by Spalding⁹ who considered the following reaction-diffusion equation:

$$\frac{\partial A}{\partial t} = \frac{\partial^2 A}{\partial \xi^2} + \beta A^n (\delta - A)^m \quad (48)$$

where the reaction term approximates the Arrhenius-type expressions for large positive values of n . Equation (48) has exact traveling wave solutions if $n=m+1$ and $m>0$. In the present study we consider the particular case where $\beta=\delta=1$, $n=1$, and $m=2$. Thus, Eq. (48) simplifies to

$$\frac{\partial A}{\partial t} = \frac{\partial^2 A}{\partial \xi^2} + A^2(1-A) \quad (49)$$

This equation has the following exact traveling wave solution:

$$A(\xi, t) = 1 / [1 + \exp(V(\xi - Vt))] \quad (50)$$

where $V=\sqrt{2}/2$, and the solutions are bounded, $0 \leq A \leq 1$. Equation (49) is to be solved subject to the following initial and boundary conditions.

$$A(\xi, 0) = 1 / [1 + \exp(V\xi)] \quad (51)$$

$$A(-\infty, t) = 1 \quad (52)$$

and

$$A(\infty, t) = 0 \quad (53)$$

In actual computations the domain $-\infty < \xi < \infty$ was truncated to the interval $-50 \leq \xi \leq 400$ and an equally-spaced grid was used in the computations. The boundaries of the truncated interval were determined by trial and error to eliminate boundary effects.

All the numerical schemes discussed before except the linear block tridiagonal method were applied to the scalar Eq. (49). The results of these schemes are shown in Figs. 1 and 2 which show the computed wave speed,

$$V_c = \int_{-\infty}^{\infty} A^2(1-A) d\xi \quad (54)$$

for two different grids. This wave speed was obtained by assuming a steady propagating traveling wave, i.e., $\partial A / \partial t = -V \partial A / \partial \xi$, and integrating Eq. (49) from $\xi = -50$ to $\xi = 400$. Figure 1 was obtained with 451 points, $\Delta t = 0.2$ and $h = 1.0$, whereas the results shown in Fig. 2 were obtained with 901 grid points, $\Delta t = 0.05$ and $h = 0.50$.

The fact that Eq. (49) has an exact solution indicates that it can be used as a test problem for numerical wave propagation studies. The results of this test are shown in Figs. 1 and 2 which present the computed wave speed as a function of time for the different numerical methods studied. It is clear from these figures that only the implicit and the majorant operator splitting methods overpredict the steady-state wave speed whereas the rest of the methods underpredict it. The large discrepancies in the wave speeds computed by the explicit and implicit methods are due to first-order truncation errors which are proportional to Δt . The explicit method of lines first overpredicts and then underpredicts the wave speed. In any event, this method is less accurate than the method of lines due to the explicit evaluation of the diffusion terms. The overprediction caused by the operator splitting method seems to be due to the second-order accurate diffusion step and, possibly, to a certain decoupling between the reaction and diffusion processes. However, the most striking feature of all these numerical schemes is that the results of the method of

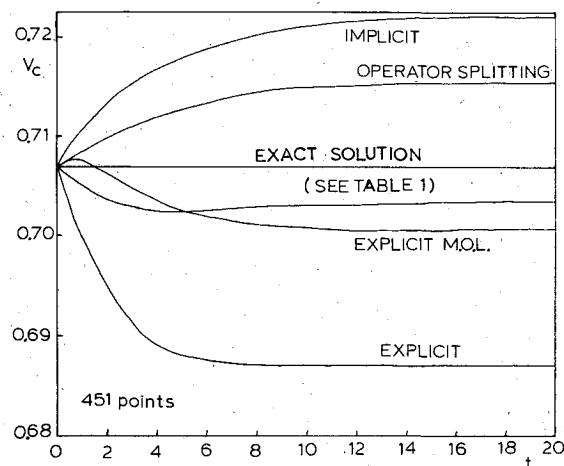


Fig. 1 Computed wave speeds as a function of time for different numerical schemes ($M=451$, $\Delta t=0.2$, $h=1.0$).

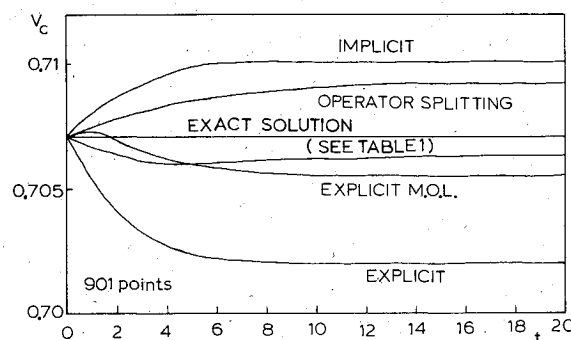


Fig. 2 Computed wave speeds as a function of time for different numerical schemes ($M=901$, $\Delta t=0.05$, $h=0.5$).

Table 1 Computed wave speeds as a function of time for different numerical schemes
($M=451$, $\Delta t=0.2$, $h=1.0$; and $M=901$, $\Delta t=0.05$, $h=0.5$)

Time	No. of Points	Quasilinear		Methods		Method of lines		Implicit predictor-corrector	
		451	901	Crank-Nicolson 451	901	451	901	451	901
0		0.7071068	0.7071068	0.7071068	0.7071068	0.7071068	0.7071068	0.7071068	0.7071068
1		0.7054866	0.7067351	0.7056002	0.7067626	0.7056644	0.7067462	0.7055016	0.7067374
2		0.7039661	0.7063855	0.7042019	0.7064293	0.7042822	0.7064048	0.7040539	0.7063924
3		0.7030459	0.7061753	0.7033763	0.7062290	0.7034507	0.7062001	0.7031970	0.7061863
4		0.7026283	0.7060810	0.7030243	0.7061410	0.7030856	0.7061094	0.7028226	0.7060950
5		0.7025187	0.7060579	0.7029583	0.7061216	0.7030060	0.7060881	0.7027402	0.7060735
6		0.7025673	0.7060711	0.7030357	0.7061374	0.7030718	0.7061023	0.7028058	0.7060880
7		0.7026836	0.7060998	0.7031713	0.7061677	0.7031979	0.7061316	0.7029328	0.7061174
8		0.7028193	0.7061328	0.7033200	0.7062018	0.7033392	0.7061648	0.7030752	0.7061509
9		0.7029509	0.7061646	0.7034606	0.7062346	0.7034741	0.7061968	0.7032113	0.7061831
10		0.7030691	0.7061931	0.7035852	0.7062638	0.7035943	0.7062254	0.7033326	0.7062120
11		0.7031711	0.7062178	0.7036919	0.7062889	0.7036974	0.7062501	0.7034368	0.7062368
12		0.7032573	0.7062386	0.7037813	0.7063101	0.7037842	0.7062709	0.7035245	0.7062578
13		0.7033292	0.7062561	0.7038558	0.7063277	0.7038564	0.7062883	0.7035973	0.7062753
14		0.7033889	0.7062706	0.7039173	0.7063425	0.7039162	0.7063028	0.7036578	0.7062899
15		0.7034382	0.7062826	0.7039683	0.7063547	0.7039657	0.7063147	0.7037078	0.7063019
16		0.7034790	0.7062926	0.7040102	0.7063647	0.7040064	0.7063246	0.7037490	0.7063120
17		0.7035127	0.7063009	0.7040448	0.7063732	0.7040401	0.7063328	0.7037831	0.7063204
18		0.7035406	0.7063077	0.7040733	0.7063800	0.7040680	0.7063396	0.7038114	0.7063272
19		0.7035639	0.7063134	0.7040970	0.7063859	0.7040911	0.7063452	0.7038347	0.7063330
20		0.7035831	0.7063182	0.7041166	0.7063906	0.7041102	0.7063498	0.7038540	0.7063379

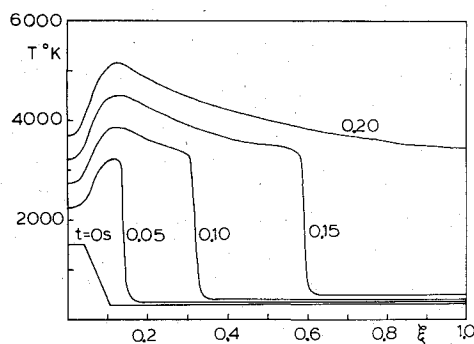


Fig. 3 Temperature profiles as a function of ξ for a laminar flame propagating in a spherical bomb.

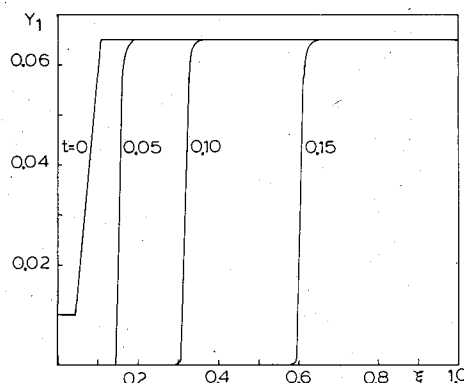


Fig. 4 Fuel mass fraction profiles as a function of ξ for a laminar flame propagating in a spherical bomb.

lines, Crank-Nicolson scheme, quasilinear method, and implicit predictor-corrector algorithm are essentially identical. The differences in the results obtained with these methods are so small that they are undistinguishable in Figs. 1 and 2. The computed wave speeds are presented in Table 1 for these four methods and for the two grids employed in the calculations reported in Figs. 1 and 2. The fact that second-order schemes such as the Crank-Nicolson and the quasilinear

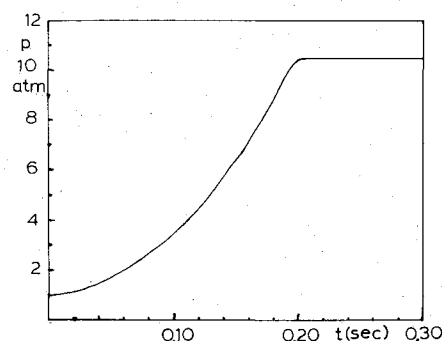


Fig. 5 Pressure profile as a function of time for a laminar flame propagating in a spherical bomb.

methods give results almost identical to those obtained with the fourth-order accurate method of lines is in excellent agreement with the conclusions reached by Reitz¹ in his studies of the ozone flame.

Propagation of Flames in Spherical Bombs

In this section we apply the numerical schemes discussed in the preceding sections to the propagation of a laminar flame in a spherical bomb. The calculations reported here were performed with a grid with 82 points, $h=0.0125$, and $\Delta t=10^{-5}$ s. The number of grid points used is, in general, not sufficient to compute the flame structure. However, the purpose here is not to predict the flame structure but to assess the efficiencies of numerical methods on the numerical treatment of the integrodifferential reaction-diffusion equations derived before. It is to be noted that the efficiencies are assessed here in terms of computation time for the same grid, geometrical configuration, chemistry, and time step. In practice, the assessment of the efficiencies should be carried out for different geometrical configurations, chemistry data including stiffness, and also different grids. In this study, however, the same time step was used because the limitation on the time step imposed by the stability considerations of the explicit method was not the controlling parameter. The time step in the present problem is controlled by the characteristic chemical time which is proportional to the inverse of the reaction rate, \dot{m}_1/ρ .

Table 2 Pressure as a function of the numerical schemes and at different times

Method/time, s	0.05	0.10	0.15	0.20
Explicit	1.78463	3.58074	6.47617	10.49360
Implicit	1.78454	3.64844	6.53219	10.25642
Crank-Nicolson	1.78457	3.64893	6.56076	10.45201
Method of lines	1.78533	3.65669	6.57578	10.49085
Explicit method of lines	1.78522	3.65568	6.57404	10.49084
Quasilinear	1.78595	3.65958	6.58869	10.50224
Linear block	1.78656	3.66346	6.59268	10.51372
Implicit predictor-corrector	1.78537	3.65699	6.57640	10.49106
Operator-splitting	1.78527	3.65584	6.57486	10.49084

In Fig. 3 we show the temperature profiles as a function of the Lagrangian coordinate ξ at different times. A flame, characterized by a very steep temperature gradient propagates from the center to the wall of the spherical bomb compressing the unburnt and burnt gases. The temperature of the unburnt gases remains uniform while that of the burnt gases increases due to adiabatic compression. In Fig. 4 we present the fuel mass fraction profiles as a function of ξ at different times. The flame front consumes the unburnt gases and behaves like a discontinuity across which the fuel mass fraction is reduced from its stoichiometric value to zero.

Figure 5 shows the pressure vs time. The pressure is a monotonically increasing function of time until the flame reaches the spherical bomb wall. Afterward, the pressure remains almost constant and the temperature becomes uniform due to the absence of chemical reactions. The nine numerical schemes used in the computation of the propagating flame give essentially identical results and their differences could not be appreciated if the results were to be plotted in Figs. 3-5. These differences are presented in Table 2 at different times. If we denote the solution obtained by the method of lines as "exact," since this method has the smallest truncation error, we observe that the explicit, implicit, and Crank-Nicolson schemes underpredict the pressure. Such underprediction is due to first-order truncation errors in the explicit and implicit methods. Both the explicit method of lines and the majorant operator splitting method slightly underpredict the solution obtained with the method of lines. The quasilinear and linear block methods overpredict the pressure values due to the linearization of the reaction terms. The results of these methods agree much better with those of the method of lines if smaller time steps are taken. For example, for the same grid and $\Delta t = 10^{-6}$ s, both the quasilinear and block methods give results which differ from those obtained with the method of lines only in the seventh decimal figure and $\Delta t = 10^{-5}$ s. This is to be expected because the flame propagation in a spherical bomb is a highly transient phenomenon, and, hence, the accuracy of the methods based on time linearization is reduced when large time steps are taken. The relative temperature differences between methods are less than 2%.

The relative efficiency of the numerical methods investigated was assessed in terms of the computer time required to achieve a specified pressure accuracy at $t = 0.15$ s. This accuracy was defined in such a way that the pressure difference between the method of lines and any other numerical method was always less than 2.5% of the pressure given by the method of lines. The relative accuracy and efficiency of the numerical methods are presented in Table 3. This table lists the accuracy and the computational time. The computational time was normalized with respect to the explicit method computation time. It should be pointed out that this definition of accuracy and efficiency is rather arbitrary. As Table 2 shows, the relative pressure differences are a function of time and they do not have a monotonic character. Table 3 shows that for a given accuracy, the explicit method is by far the most efficient, whereas the linear block tridiagonal algorithm is the least. This is to be expected owing to the dependence of pressure on ϕ which requires the introduction of an iterative

Table 3 Normalized computational times

Method	Relative accuracy, %	Normalized computation time ^a
Explicit	-1.51	1.00
Implicit	-0.66	1.81
Explicit method of lines	-0.03	1.86
Crank-Nicolson	-0.23	1.90
Method of lines	0.00	1.91
Quasilinear	0.20	1.93
Operator-splitting	-0.01	2.60
Implicit predictor-corrector	0.01	2.97
Linear block	0.26	3.07

^aUnity corresponds to computations performed with an 82-point grid up to $t = 0.15$ s, and is equal to 1043 s of CPU time on a DEC-20 computer.

algorithm in the linear block method. Besides, the method also requires the inversion of a block tridiagonal matrix which is a more costly task than the inversion of a tridiagonal matrix. This difference accounts for the relatively faster quasilinear method. A striking feature of this table is that the quasilinear method is less efficient than the implicit and Crank-Nicolson schemes despite the time linearization. In fact, the numerical results indicate that this difference is due to the evaluation of the Jacobian matrix ($\partial S / \partial A$) [see Eq. (43)] which contains several exponential terms [see Eq. (20)] which have been evaluated analytically. The large computational times required by the operator splitting and implicit predictor-corrector methods are due to the fact that these methods involve two steps; e.g., the predictor is an explicit method of lines, and the corrector step involves the inversion of a tridiagonal matrix, hence, they are slower than the method of lines as well as the explicit method of lines. Furthermore, all the methods shown in Table 3 except the explicit method require iterations which slow convergence. In these calculations convergence within the time step was based on the following criteria.

$$|p^{(k+1)} - p^{(k)}| / p^{(k)} \leq 10^{-4}$$

and

$$|T_i^{(k+1)} - T_i^{(k)}| / T_i^{(k)} \leq 10^{-4}$$

Table 3 also shows that for an 82-point grid and $\Delta t = 10^{-5}$ s the efficiency of a fourth-order accurate method of lines is comparable to that of the first-order accurate implicit method. In any event, a fourth-order method for the present problem is slower by a factor of approximately 1.90 than the fastest explicit method.

Conclusions

Nine finite difference schemes which use second-order spatial approximations have been developed and applied to solve a reaction-diffusion equation which has an exact traveling wave solution, and to study the propagation of a laminar flame in a spherical bomb. The results of these in-

vestigations show that, for the reaction-diffusion equation, the first-order truncation errors of the explicit and implicit methods cause an underprediction and overprediction of the steady-state wave speed, respectively. The accuracy of the explicit method of lines is somewhat deteriorated by the explicit evaluation of the diffusion terms, whereas that of the operator splitting method depends very much on the time and space steps. For the same space step, large time steps uncouple the diffusion and reaction processes and eventually lead to complete instability. Perhaps the most striking feature of the reaction-diffusion problem is that the second-order accurate quasilinear, Crank-Nicolson, and implicit predictor-corrector methods give essentially the same answer as that of a fourth-order accurate method of lines.

The investigation of laminar flame propagation in a spherical bomb shows similar results to those found with the reaction-diffusion equation but, in addition, it shows that the explicit method is far more efficient than the other eight numerical methods. However, the explicit method is also the least accurate scheme for the same time step. The least efficient method is the linear block tridiagonal algorithm. This method, as well as the quasilinear scheme, is not very efficient because of the iterative procedure required. This iteration procedure is due to the assumption of a time-dependent uniform pressure throughout the spherical bomb, otherwise the execution of both the quasilinear and linear block algorithms would be very fast since, in general, their linearization produces a set of linear equations whose solution

does not require iterations. It has also been found that fourth-order accurate schemes, like the method of lines, can be as efficient as first-order implicit schemes.

References

- ¹Reitz, R. D., "The Application of an Explicit Numerical Method to a Reaction-Diffusion System in Combustion," unpublished manuscript, 1980.
- ²Otey, G. R. and Dwyer, H. A., "A Numerical Study of the Interaction of Fast Chemistry and Diffusion," *AIAA Journal*, Vol. 17, June 1979, pp. 606-613.
- ³Ramos, J. I., "A Numerical Study of One-Dimensional Enclosed Flames," *Numerical Properties and Methodologies in Heat Transfer*, Hemisphere Pub. Co., Washington, D.C., 1983, pp. 529-546.
- ⁴Williams, F. A., *Combustion Theory*, Addison-Wesley, Reading, Mass., 1965, pp. 1-17.
- ⁵Yannenkov, N. N., *The Method of Fractional Steps*, Springer Verlag, New York, 1971, pp. 17-41.
- ⁶Hornbeck, R. W., "Numerical Marching Techniques for Fluid Flows with Heat Transfer," NASA SP-297, 1973, pp. 301-305.
- ⁷Bellman, R. E. and Kalaba, R., *Quasilinearization and Nonlinear Boundary Value Problems*, American Elsevier, New York, 1965, pp. 111-124.
- ⁸Briley, R. M. and McDonald, H., "Solution of the Multidimensional Compressible Navier-Stokes Equations by a Generalized Implicit Method," *Journal of Computational Physics*, Vol. 24, Aug. 1977, pp. 372-392.
- ⁹Spalding, D. B., "II. One-Dimensional Laminar Flame Theory for Temperature-Explicit Reaction Rates," *Combustion and Flame*, Vol. 1, Sept. 1957, pp. 296-307.

From the AIAA Progress in Astronautics and Aeronautics Series . . .

VISCOUS FLOW DRAG REDUCTION—v. 72

Edited by Gary R. Hough, Vought Advanced Technology Center

One of the most important goals of modern fluid dynamics is the achievement of high speed flight with the least possible expenditure of fuel. Under today's conditions of high fuel costs, the emphasis on energy conservation and on fuel economy has become especially important in civil air transportation. An important path toward these goals lies in the direction of drag reduction, the theme of this book. Historically, the reduction of drag has been achieved by means of better understanding and better control of the boundary layer, including the separation region and the wake of the body. In recent years it has become apparent that, together with the fluid-mechanical approach, it is important to understand the physics of fluids at the smallest dimensions, in fact, at the molecular level. More and more, physicists are joining with fluid dynamicists in the quest for understanding of such phenomena as the origins of turbulence and the nature of fluid-surface interaction. In the field of underwater motion, this has led to extensive study of the role of high molecular weight additives in reducing skin friction and in controlling boundary layer transition, with beneficial effects on the drag of submerged bodies. This entire range of topics is covered by the papers in this volume, offering the aerodynamicist and the hydrodynamicist new basic knowledge of the phenomena to be mastered in order to reduce the drag of a vehicle.

456 pp., 6 × 9, illus., \$25.00 Mem., \$40.00 List

TO ORDER WRITE: Publications Dept., AIAA, 1290 Avenue of the Americas, New York, N.Y. 10104